

New, low-energy excitations in ^{107}Mo and ^{109}Mo W. Urban,¹ T. Rząca-Urban,¹ J. Wiśniewski,¹ J. Kurpeta,¹ A. Płochocki,¹ J. P. Greene,² A. G. Smith,³ and G. S. Simpson³¹*Faculty of Physics, University of Warsaw, ulica Pasteura 5, PL-02-093 Warsaw, Poland*²*Argonne National Laboratory, Argonne, Illinois 60439, USA*³*Department of Physics and Astronomy, The University of Manchester, M13 9PL Manchester, United Kingdom*

(Received 6 November 2019; accepted 29 July 2020; published 14 August 2020)

New ground-state level with spin-parity $1/2^+$ is established in ^{109}Mo , 69.8 keV below the previously reported $5/2^+$ ground state in this nucleus, based on precise spectroscopy measurements of γ radiation following spontaneous fission of ^{248}Cm performed using the Eurogam2 array of anti-Compton spectrometers. Analogous measurement of γ radiation following spontaneous fission of ^{252}Cf , performed using the Gammasphere array, confirms the new $1/2^+$ ground state of ^{107}Mo , proposed recently and establishes the isomeric character of the $5/2^+$ first excited state in ^{107}Mo . Two β -decaying isomers are suggested in ^{111}Mo nucleus based on regular energy systematics, supporting previous predictions. Low-energy excitations in Mo isotopes are interpreted and compared to calculations reported in the literature. The results suggest shape transition from prolate to oblate deformation at $N \geq 67$.

DOI: [10.1103/PhysRevC.102.024318](https://doi.org/10.1103/PhysRevC.102.024318)

I. INTRODUCTION

A recent study of low-spin levels in ^{107}Mo , populated in β^- decay of ^{107}Nb has revealed a new ground state located 65.4 keV below the previously proposed ground state in this nucleus [1]. In the past, the ground state of ^{107}Mo was assigned spin-parity $3/2^+$ [2], then, $7/2^-$ [3], and later $5/2^+$ [4]. The new ground state is assigned spin-parity $1/2^+$ based on the $E2$ multipolarity of the 65.4-keV transition [1,5], which deexcites the $5/2^+$ level previously proposed as the ground state and now placed at 65.4 keV [1].

An isomer in ^{107}Mo with a half-life of 245(15) ns was first reported at 66.3 keV [6]. In Ref. [3], this level was assigned a tentative spin-parity $5/2^-$. Subsequently, a 65.4-keV transition was observed in ^{107}Mo deexciting an isomer with a half-life of 420 ns [5]. It was proposed that this transition deexcites a $1/2^+$ isomer located 65.4 keV above the ground state [5]. With the new $1/2^+$ ground state of ^{107}Mo , proposed in Ref. [1], the 420-ns isomer should correspond to the $5/2^+$, 65.4-keV excited level in this nucleus [1], although the isomeric character of the 65.4-keV level was not verified in Ref. [1].

A similar scenario may be expected in the ^{109}Mo nucleus. Its ground state that was first assigned spin-parity $(7/2^-)$ [3] was later interpreted as the $5/2^+$ configuration, analogous to that in ^{107}Mo [4]. Subsequently, an isomer with a half-life of 194 ns was reported in ^{109}Mo at 70 keV [7]. By analogy with the 420-ns isomer in ^{107}Mo , the 70-keV isomeric transition in ^{109}Mo was proposed to be a stretched $E2$, deexciting spin-parity $(1/2^+)$ isomer to the $5/2^+$ ground state [7]. As suggested in Ref. [1], the isomeric transition in ^{109}Mo may deexcite the present $5/2^+$ ground state in ^{109}Mo defining a new ground state with spin-parity $1/2^+$, located 70 keV below this $5/2^+$ level.

In this paper, we reinvestigated both ^{107}Mo and ^{109}Mo nuclei produced in spontaneous fission of ^{248}Cm and ^{252}Cf in order to verify their ground states and isomers as well as some unexplained properties reported in Ref. [5]. We start in Sec. II with predictions based on systematics. Then, the measurement and the obtained results are presented in Sec. III. The results are discussed in Sec. IV, which is followed by a summary in Sec. V.

II. NEW LEVELS EXPECTED IN $^{107,109}\text{Mo}$

Our recent works [8,9] demonstrated remarkably regular systematics of excitation energies in odd- A nuclei of the $A \approx 110$ region. Such systematics may help predicting new excitations and other properties of $^{107,109}\text{Mo}$, in particular, spin and parity of the ground state in ^{109}Mo .

In even-even nuclei, one often uses “stable,” complex ground-state structures as the reference for systematics of excitation energies. This is especially useful when tracing collective excitations built on top of ground states as demonstrated in our recent work [10]. In contrast, ground states of odd- A nuclei are usually dominated by single-particle (s.p.) configurations (Nilsson orbitals in deformed nuclei), which can change rapidly when varying proton (isotones) or neutron (isotopes) numbers. Therefore, the ground state of an odd- A nucleus may not be a good reference. Instead, one should use a level dominated by an orbital, which does not mix with other orbitals. A reasonable choice is a level dominated by the highest- Ω subshell of the intruder shell.

Figure 1 shows schematically how this works for $A \approx 110$ isotones where the intruder is the $h_{11/2}$ neutron shell and the reference is a $11/2^-$ level dominated by the $\nu 11/2^- [505]$ orbital. Other prominent levels in these isotones are due to

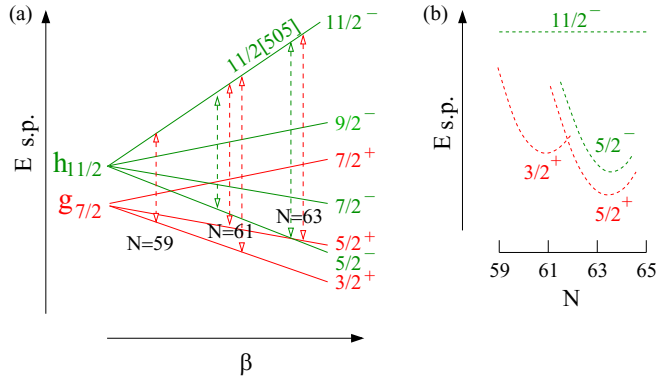


FIG. 1. Schematic explanation of regular energy systematics observed in the $A \approx 110$ mass region. See the text for further comments.

subshells of the $\nu g_{7/2}$ shell (in the simplified picture of Fig. 1(a) we show the splitting between Nilsson orbitals due to the spin-orbit interaction only, neglecting mixing of $\nu g_{7/2}$ subshells with other positive-parity orbitals). In the $A \approx 110$ isotones, the deformation β grows with the increasing neutron number and the splitting between Nilsson orbitals grows accordingly. At $N = 59$ where the Fermi level approaches the $3/2^+$ orbital the difference between s.p. energies ($E_{s.p.}$) of the $3/2^+$ and $11/2^-$ orbitals [marked by an arrow in Fig. 1(a)] is smaller than at $N = 61$ where the odd neutron already occupies the $3/2^+$ orbital. At $N = 63$, the odd neutron occupies the $5/2^+$ orbital and the $3/2^+$, populated by a couple of paired neutrons, is “buried” in the core. Exciting the $3/2^+$ (hole) level at $N = 63$ costs more energy. Consequently, the excitation energy of the $3/2^+$ level will increase, and the distance between $3/2^+$ and $11/2^-$ levels will decrease. This is depicted in Fig. 1(b) by the $3/2^+$ “parabola.” At higher neutron numbers, the same scenario applies to the $5/2^+$ and $5/2^-$ levels, illustrated by corresponding parabolas in Fig. 1(b).

Experimental systematics drawn in Fig. 2 for several Mo, Ru, and Pd isotopes from the $A \approx 110$ region, indeed, reveal such parabolic trends for both, positive- [Fig. 2(a)] and negative-parity [Fig. 2(b)] levels. To the right-hand side of Figs. 2(a) and 2(b), we have redrawn these parabolas, starting at the common origin. All have remarkably similar shapes and a “half-width” of about two particles, which corresponds to filling a single Nilsson orbital.

Extrapolating the parabola for the $1/2^+$ levels to $N = 67$ as shown in Fig. 2(a), suggest that the $1/2^+$ level in $^{109}\text{Mo}_{67}$ may occur a few dozens of keV below the $5/2^+$ level [“ $1/2^+$ expected,” open dashed circle in Fig. 2(a)] rather than 70 keV above the $5/2^+$ level as suggested by Kameda *et al.* [7].

Similarly, the parabola corresponding to the $5/2^-$ [532] orbital, when extrapolated to $N = 65$ as shown in Fig. 2(b), suggests that, in $^{107}\text{Mo}_{65}$, this $5/2^-$ excitation (open, dashed circle) may occur a few dozens of keV below the $7/2^-$ level. Such a possibility was suggested by calculations of ^{107}Mo in Ref. [5].

It is interesting to note that excited levels calculated for odd- A nuclei of this region display similar parabolic trends. Figure 3 shows excitations in Zr and Mo isotones calculated within the Hartree-Fock-Bogoliubov plus the equal-filling-

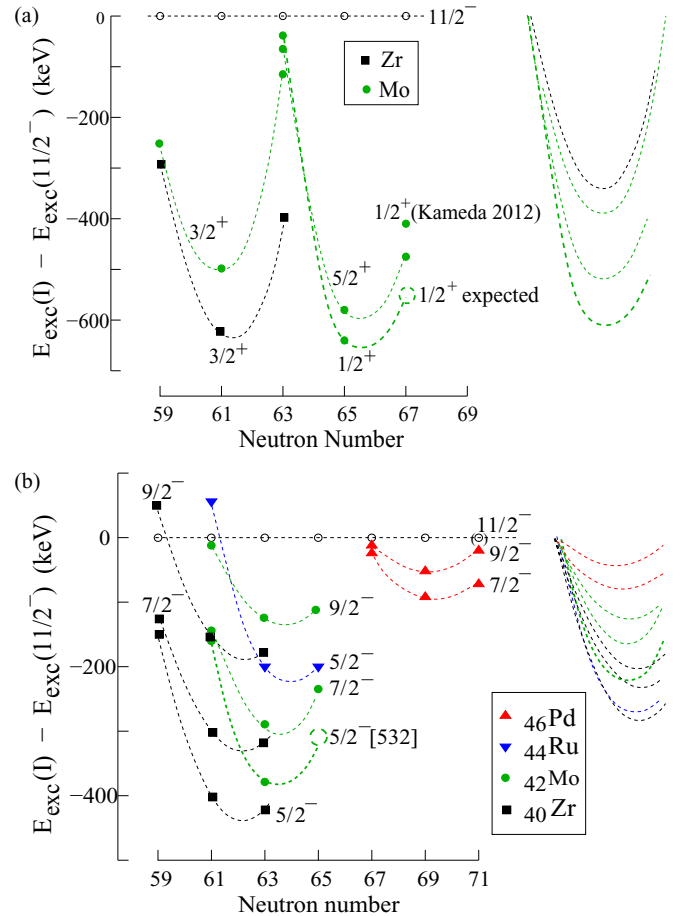


FIG. 2. Experimental excitation energies of low-spin levels of (a) positive and (b) negative parities, in odd- A Zr, Mo, Ru, and Pd isotopes. The data are taken from Refs. [1,4,5,7–9,11,12]. Lines are drawn to guide the eye. See the text for further explanations.

approximation method [13]. The results reported in Figs. 4 and 5 of Ref. [13] are redrawn in Fig. 3 to show excitations relative to the calculated $11/2^-$ level. This theoretical systematics will be commented on further in Sec. IV.

III. MEASUREMENTS AND RESULTS

New experimental information on ^{107}Mo and ^{109}Mo obtained in this paper results from the analysis of γ radiation following spontaneous fission of ^{248}Cm and ^{252}Cf , measured using the Eurogam2 [14] and Gammasphere [15] arrays, respectively. The experiments and data-analysis techniques were described in previous papers (see, e.g., Refs. [16,17]). Compared to the Eurogam2 measurement of ^{248}Cm used in the previous analysis of ^{107}Mo [4] and ^{109}Mo [18], the Gammasphere measurement provided about an order of magnitude more triple- γ events, allowing the observation of weaker effects in ^{107}Mo . Important for the present paper was that the hardware time window of the Gammasphere measurement was wider (900 ns) than that in the Eurogam2 measurement (400 ns), allowing better discrimination against isomeric transitions. In the present paper, we still used the data from the

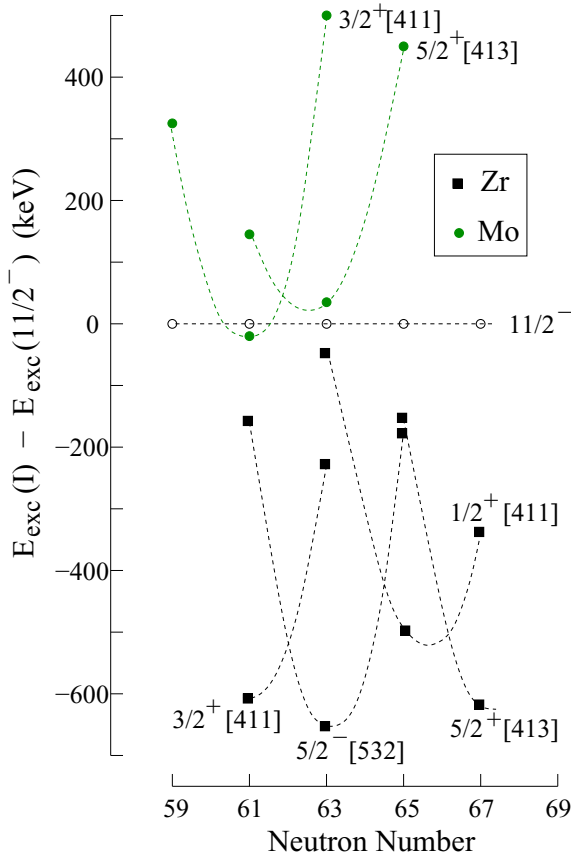


FIG. 3. Calculated excitation energies of low-spin excitations in odd-A, Zr, and Mo isotopes. The data are based on Ref. [13]. Lines are drawn to guide the eye. See the text for further explanations.

^{248}Cm fission measurement because this reaction populates the ^{109}Mo nucleus more than fission of ^{252}Cf and provides cleaner spectra. Compared to Ref. [4], in the present paper, we sorted new specific three-dimensional (3D) histograms for the ^{248}Cm fission data, allowing better timing analysis. We also note that using two different fissioning systems provided better discrimination against contaminating effects.

A. $5/2^+$ isomeric state in ^{107}Mo

Figure 4(a) shows a low-energy fragment of a doubly gated γ -ray spectrum obtained from the 3D *ggg* histogram where triple- γ events were sorted within the full 900-ns time window of the ^{252}Cf measurement. The spectrum is gated on the 348.3- and 110.4-keV lines of the negative-parity cascade in ^{107}Mo [4]. In the spectrum, one sees a strong 123.5-keV line, corresponding to the next transition in this cascade and a weak line at 65.4 keV. An analogous spectrum displayed in Fig. 4(b), which is gated on the 152.3- and 306.4-keV transitions of another cascade in ^{107}Mo [4], shows again the two lines at 123.5 and 65.4 keV. Thus, the present work confirms the placement of the 65.4-keV transition in cascade with the 152.3- and 348.3-keV transitions, which is located below them and depopulates the $5/2^+$ level.

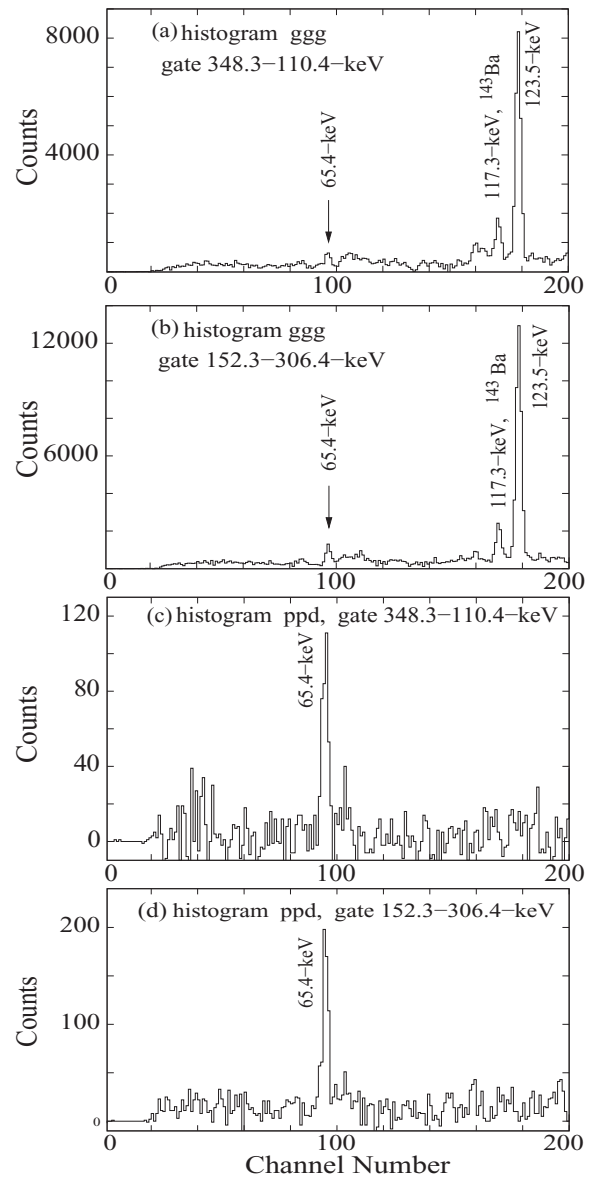


FIG. 4. Doubly gated γ -ray spectra for ^{107}Mo obtained in this paper from ^{252}Cf fission data. See the text for further comments.

As suggested in Ref. [1], the 65.4-keV, ground-state transition reported may be the same as the 65.4-keV isomeric transition reported in Ref. [5]. Consequently, the 420-ns half-life should be assigned to the $5/2^+$ level. Because of experimental limitations, the isomeric nature of the $5/2^+$ level was not verified in Ref. [1] but can be confirmed in the present paper. The isomeric character of the 65.4-keV transition depopulating the $5/2^+$ level in ^{107}Mo is highlighted in Figs. 4(c) and 4(d), which show doubly gated γ spectra obtained from the 3D *ppd* histogram. This histogram was sorted with specific timing conditions where energy signals on both *p* (“prompt”) axes were collected within a narrow time window extending from -22 to 22 ns and energy signals on the *d* (“delayed”) axis were collected within a delayed time window extending from 400 to 800 ns relative to “time zero” defined by the master trigger signal of Gammasphere. The delay of the delayed

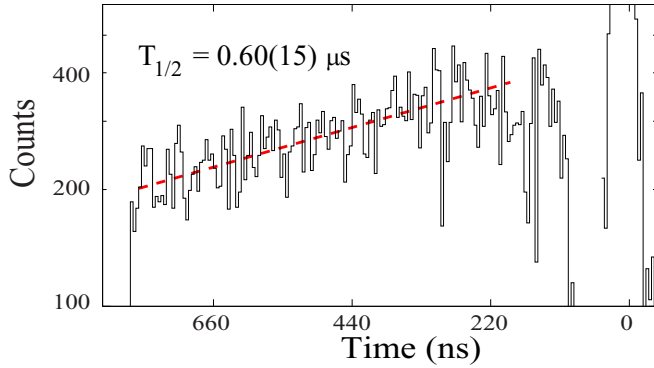


FIG. 5. Time-delayed spectrum, doubly gated on the 348.3- and 65.4-keV lines in the ^{252}Cf fission data. The dashed (red) line represents the exponential fit to the data.

window was sufficient to avoid the so-called time jitter caused by worse timing response of Ge detectors at low- γ energies. The two spectra shown in Figs. 4(c) and 4(d) were doubly gated on prompt- γ lines and are displayed along the delayed axis.

The half-life of the 65.4-keV level was obtained in this paper from the time-delayed spectrum, shown in Fig. 5. The spectrum is doubly gated on the prompt 348.3-keV and the delayed 65.4-keV γ lines and shows the difference between time signals corresponding to the two γ lines. The obtained half-life, corresponding to the slope marked by the (red), dashed line in Fig. 5 is $0.60(15) \mu\text{s}$, in accord with the half-life reported in Ref. [5].

Using γ intensities of the 65.4- and 348.3-keV transitions, seen in the γ -ray spectrum doubly gated on the 110.4- and 123.5-keV transitions, we estimated the total conversion coefficient of the 65.4-keV transition to be $6.0(1.5)$, which agrees with the theoretical total conversion coefficients of 5.6 calculated for an $E2$ transition of this energy [19].

B. $5/2^-$ state in ^{107}Mo

Figure 6 shows two spectra which illustrate the presence of a new, $5/2^-$ level in ^{107}Mo . The spectra were obtained from the ggg histogram of triple- γ coincidences, sorted within the full 400-ns time window of the ^{248}Cm measurement. In Fig. 6(a), we show a γ -ray spectrum doubly gated on the known 123.5-keV line of ^{107}Mo [4] and the 299.4-keV line, depopulating the 364.7-keV level proposed in ^{107}Mo [1] with a tentative $(5/2, 7/2)$ spin assignment. The spectrum shows, among others, a γ line at 159.6 keV. We propose that this line corresponds to a new transition in ^{107}Mo , which links the 524.1- and 364.7-keV levels. Further gating confirms this link as well as the 147.0-keV decay of the 364.7-keV level, reported in Ref. [1].

The presence of the 110.4-keV line in Fig. 6(a) indicates that there is also a new 49.0-keV link between the 413.7- and the 364.7-keV levels. The 49.0-keV line is barely seen in Fig. 6(a) because of its low- γ intensity. However, the spectrum displayed in Fig. 6(b) with gates set at 49 and 299 keV shows clearly the 110.4-, 123.5-, and 233.8-keV lines, confirming the 49.0-299.4-keV cascade in ^{107}Mo . Considering

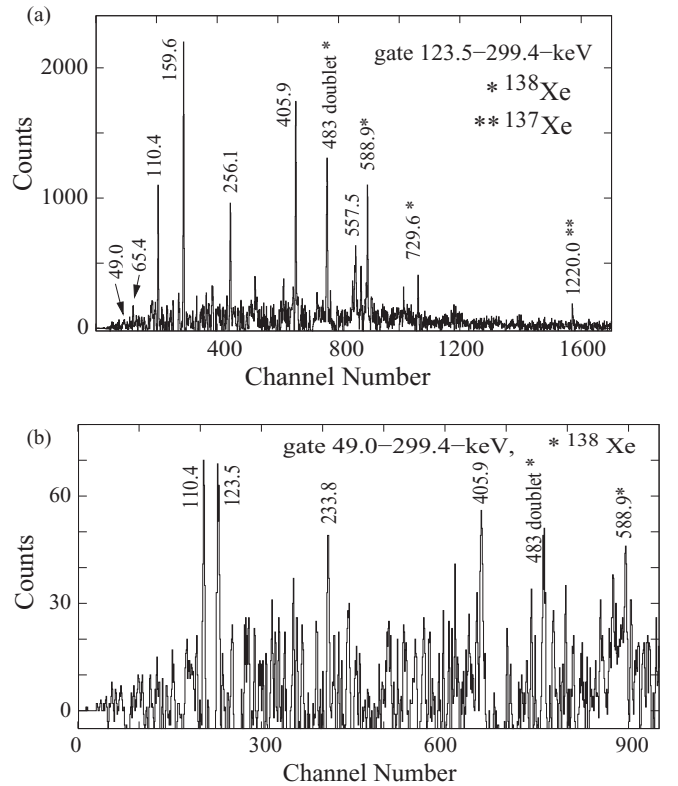


FIG. 6. Doubly gated γ -ray spectra obtained in this paper from the ggg histogram sorted out of triple- γ coincidences following ^{248}Cm fission. The spectra show the known Ref. [4] and the new 49.0- and 65.4-keV lines of ^{107}Mo . γ lines are labeled with their energies in keV. See the text for more comments.

the observed decay branchings, shown in Table I, and the known spins in ^{107}Mo , we propose spin-parity $5/2^-$ for the 364.7-keV level.

C. $1/2^+$ ground state in ^{109}Mo

Figure 7 shows a γ -ray spectrum doubly gated on the 111.0- and 222.2-keV, known lines of ^{109}Mo [18] in the ppd histogram sorted out of triple- γ events from ^{248}Cm fission using the (0–30)-ns prompt p and (200–400)-ns delayed d -time windows. The spectrum clearly shows that the 69.8-keV transition is in one cascade with the gating transitions. We propose that this is the same transition as the 70-keV isomeric

TABLE I. Relative γ intensities, I_γ for new levels and transitions in ^{107}Mo as observed in this paper.

Level (keV)	E_γ (keV)	I_γ (rel.)
364.7	147.0	10(5)
	299.4	100(6)
413.7	49.0	4(2)
	196.1	5(2)
	348.3	100(5)
524.1	110.4	80(4)
	159.6	14(2)
	306.4	100(4)

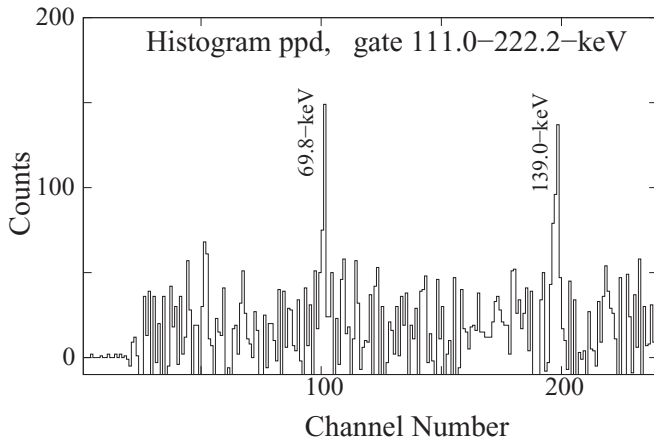


FIG. 7. Doubly gated γ -ray spectrum for ^{109}Mo , obtained in this paper from the *ggg* histogram sorted out of triple- γ coincidences following ^{248}Cm fission. See the text for more comments.

transition reported in Ref. [7] because Fig. 7 suggests that the 69.8-keV transition depopulates an isomer. This could not be determined with certainty in the present paper due to the insufficient timescale of the ^{248}Cm fission measurement (possible contamination by the jitter effect), whereas in our ^{252}Cf fission data, the ^{109}Mo nucleus is not populated strongly enough to allow the observation of the 69.8-keV line.

The coincidence relation of the 69.8-keV transition with the 111.0–222.2-keV cascade indicates that this transition depopulates the $5/2^+$ level, considered, so far, to be the ground state of ^{109}Mo [18] and populates a new ground state. To the new ground state, we tentatively assign spin-parity $1/2^+$, considering the isomeric character of the 69.8-keV transition consistent with the $E2$ multipolarity.

D. Low-energy excitation schemes of ^{107}Mo and ^{109}Mo

Figure 8 shows partial level schemes of (a) ^{107}Mo and (b) ^{109}Mo with the new $1/2^+$ ground states and other new levels and transitions. Table I shows γ branching for the new levels and levels with new decays in ^{107}Mo as observed in this paper. Other intensities can be found in Refs. [4,18].

In ^{107}Mo , we have included a fragment of the known band comprising the 66.0-, 99.4-, and 165.4-keV transitions [4], which now forms the ground-state band [1] as well as the 543.8-keV level reported with a tentative $(7/2^+)$ spin parity [1]. In this paper, we have searched unsuccessfully for a cascade on top of the 543.8-keV level. Therefore, considering the argument of the yrast population in fission process [20], one would rather propose lower spin for this level as suggested in Fig. 8.

In Ref. [21], a γ -vibrational band was proposed in ^{107}Mo on top of the $7/2^-$ [523] neutron configuration. Considering the new $5/2^-$ level at 364.7 keV in ^{107}Mo proposed in this paper, the negative-parity band in ^{107}Mo may be based on the $5/2^-$ [532] neutron configuration, and one may expect a γ vibration coupled to this level. This would produce an in-band $9/2^-$ level below the $11/2^-$ level at 949.8 keV, reported in Ref. [21]. In this paper, we do observe the band based on

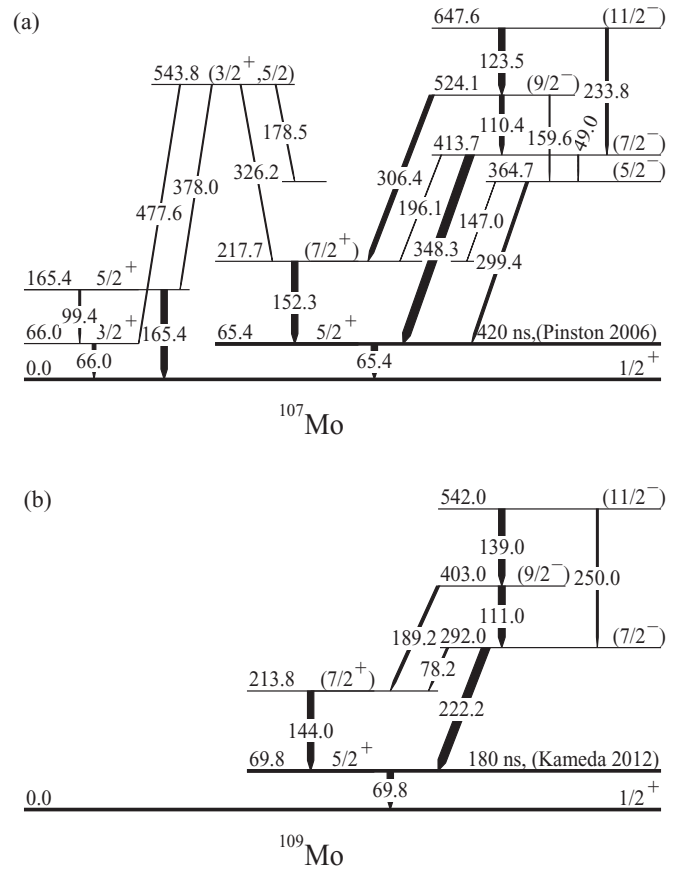


FIG. 8. Low-energy parts of excitation schemes of ^{107}Mo and ^{109}Mo . The data are taken from this paper and Refs. [1,4,5,7,18].

the 949.8-keV level [21] but could not find any in-band $9/2^-$ level, below the 949.8-keV level. A possible reason may be the unfavored nature of the $5/2^-$ level in the negative-parity band.

In ^{109}Mo , one may expect a band on top of the new $1/2^+$ ground state, analogous to the $1/2^+$ ground-state band in ^{107}Mo . In the present paper, we could not find any candidate for such a ground-state band in ^{109}Mo , probably because of too low statistics of our data. Identification of such a band is of prime importance for verifying whether the $1/2^+$ ground states in ^{107}Mo and ^{109}Mo correspond to the same Nilsson configuration. A dedicated β -decay experiment may help here.

IV. DISCUSSION

A. Interpretation of excitations in Mo isotopes

The new excitation schemes of ^{107}Mo and ^{109}Mo allow better energy systematics to be built and used for predicting properties of more neutron-rich isotopes. Furthermore, comparing such broad experimental systematics to the calculated systematics imposes stronger constraints on theoretical models than the comparisons for individual nuclei. New level schemes of $^{107,109}\text{Mo}$ offer also better understanding of the

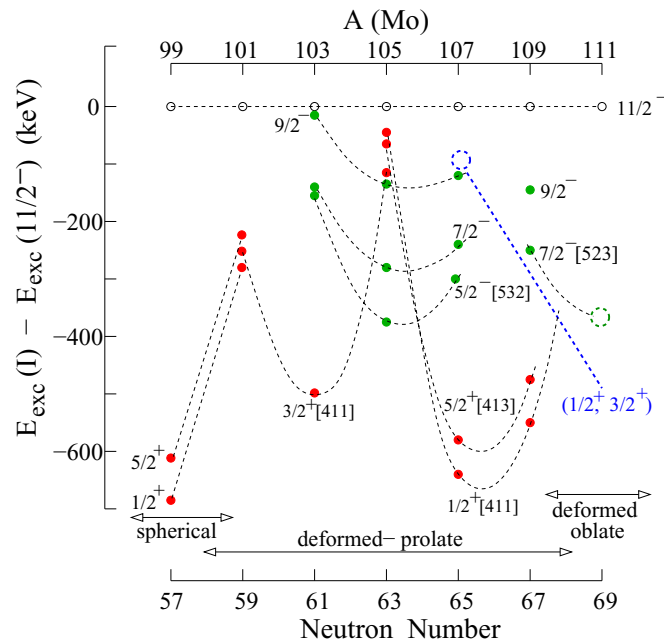


FIG. 9. Excitation energies of selected low-spin excitations in odd-Mo isotopes for positive (red) and negative (green) states. The data are taken from this paper and Refs. [1,4,5,7–9,11,12]. Lines are drawn to guide the eye. See the text for further explanations.

structure of their $A = 107$ and $A = 109$ isobars, connected by β^- decays.

Figure 9 shows the experimental systematics of low-energy excitations, drawn relative to the $11/2^-$ level for odd- A neutron-rich molybdenum isotopes. There are three characteristic regions in this systematics. In isotopes up to $^{101}\text{Mo}_{59}$, one observes spherical s.p. excitations corresponding to the $s_{1/2}$ and $d_{5/2}$ neutron shells, which approach quickly the $h_{11/2}$ shell when the neutron number grows. Analogous systematics of calculated excitation energies [13], drawn in Fig. 10 relative to the $11/2^-$ excitations, also shows such a rapid increase.

From ^{101}Mo up extends the region of prolate-deformed nuclei with characteristic parabolas corresponding to the population of subsequent Nilsson orbitals. It starts with the $3/2^+[411]$ orbital in ^{101}Mo and ^{103}Mo , through the $5/2^-[532]$ orbital in ^{105}Mo to the $5/2^+[413]$ orbital in $^{107,109}\text{Mo}$. We note that the $5/2^+[413]$ configuration, identified in ^{107}Mo in Ref. [4] fits well the experimental systematics and is also reported in ^{107}Mo in the calculations of Refs. [5,13]. Therefore, the $5/2^+[402]$ configuration mentioned in ^{107}Mo by Ref. [22] is probably a misprint. The three Nilsson orbitals seen in Fig. 9 are also seen in Fig. 10, although at higher energies relative to the $11/2^-$ level. This gives hints towards possible improvements of the calculations reported in Ref. [13].

The parabolic trend shown by the new $1/2^+$ levels in ^{107}Mo and ^{109}Mo , which follow the $5/2^+[413]$ orbital, suggest that these $1/2^+$ levels may correspond to the $1/2^+[411]$ Nilsson orbital located just above the $5/2^+[413]$ orbital on the prolate side (see, e.g., Fig. 9 in Ref. [23]). As seen in Fig. 10, the calculations of Ref. [13] favor the $1/2^+[420]$ oblate Nilsson orbital for the configuration of the ground state in ^{107}Mo (the

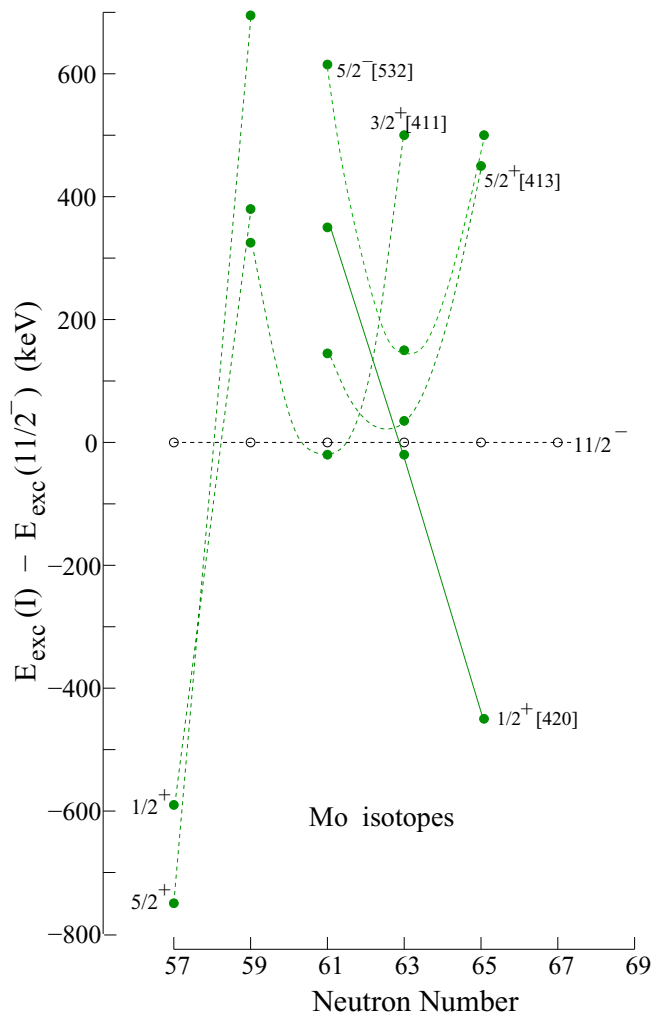


FIG. 10. Calculated levels in Mo isotopes. The data are based on Ref. [13]. Lines are drawn to guide the eye. See the text for further explanations.

$1/2^+[420]$ oblate orbital is also calculated as the ground state in ^{105}Mo). Therefore, it is important to verify the nature of ground states in ^{107}Mo and ^{109}Mo nuclei.

The similar nature of the new $1/2^+$ ground states in ^{107}Mo and ^{109}Mo is supported by similar populations of excited levels in ^{107}Tc and ^{109}Tc , observed in β^- decays of the two Mo isotopes, respectively, as seen in Table II and Fig. 7 of Ref. [24]. In Ref. [24], this was attributed to the same $5/2^+$ configuration of both ground states in ^{107}Mo and ^{109}Mo . The present paper indicates that this may be due to the same $1/2^+$ configuration of the two Mo isotopes. Interestingly, spin-parity $1/2^+$ of the ground states in ^{107}Mo and ^{109}Mo allows to improve the spin-parity assignments to levels in ^{107}Tc and ^{109}Tc for which various hypotheses were considered in Ref. [24].

The “mechanism” of Fig. 1 works in the region marked deformed in Fig. 9 where one observes prolate-deformed configurations displaying parabolic dependence in function of N . Above $N = 69$, this may look different because one expects, here, the dominance of oblate Nilsson configurations.

The calculations of Ref. [13] shown in Fig. 10 predict the transition to this third region (oblate deformation) already at $N = 63$ (the $1/2^+[420]$ oblate orbital) whereas the experiment (Fig. 9) suggests such a transition above $N = 67$. An analogous transition to oblate deformation was recently observed experimentally in Pd isotopes above $N = 67$ (see Fig. 6 in Ref. [9]).

The extrapolation of the parabolic trend for the $1/2^+[411]$ and $7/2^+[523]$ prolate configurations to $N = 69$ in Fig. 9 suggests that at $N = 69$ the $7/2^- [523]$ level may be located below the $1/2^+[411]$ level in the prolate potential. However, the ground state of ^{111}Mo may be formed by an oblate configuration, located below the prolate $7/2^- [523]$ level as shown in Fig. 9 by the thick, (blue) dashed line. The inspection of the Nilsson diagram for neutrons in this mass region [23] shows the presence of the $1/2^+[420]$ and $3/2^+[422]$ oblate configurations at $N = 69$. It is of high interest to search for such excitations in ^{107}Mo and ^{109}Mo in order to see their evolution with the neutron number, which may tell what is the ground state of ^{111}Mo . As mentioned above, the 543.8-keV level in ^{107}Mo [marked by the (blue) dashed circle in Fig. 9] may have spin $3/2^+$. If the prediction sketched in Fig. 9 is confirmed, ^{111}Mo may have two β -decaying isomers. Such a possibility was also proposed in our previous work [25] where we observed excited levels in ^{111}Tc with spins ranging from $1/2$ to $11/2$, populated in the β^- decay of ^{111}Mo .

B. γ deformation in Mo isotopes

The value of γ deformation in odd- A , neutron-rich Mo isotopes should be verified considering the new $1/2^+$ spin-parity assignments to ground states in ^{107}Mo and ^{109}Mo . In Ref. [5], a value of $\gamma = 16.5^\circ$ for the triaxial deformation in ^{107}Mo was deduced by comparing quasiparticle rotor model calculations to the available experimental data. The γ values for ^{106}Mo and ^{108}Mo shown in Table V of Ref. [5] indicate an increase with the neutron number. Considering the γ value of 17° obtained in Ref. [5] for ^{105}Mo one would expect the γ deformation in ^{107}Mo to be larger than 16.5° . This is also suggested by γ values reported in the neighboring nuclei as listed in Table II. The general trend seen in Table II is the increase in the γ value with the increasing proton and neutron numbers. One also notes that, on average, the γ value at $N = 65$ is higher than 16.5° .

Figure 11 shows the energies of excited levels in ^{105}Mo and ^{107}Mo calculated in Ref. [5] for various γ deformations (open symbols). The $5/2^-$ excitation energy decreases relative to the $5/2^+$ energy in ^{105}Mo with the increasing γ deformation. When a linear extrapolation is applied, the reproduction of the experimental $5/2^-$ level (filled circle) suggests $\gamma \approx 25^\circ$. A similar decrease in energy is seen for the $1/2^+$ level in ^{105}Mo . Again, linear extrapolation to the experimental energy suggests $\gamma \approx 25^\circ$. Similar trends applied to levels in ^{107}Mo reproduce the energy of the new $1/2^+$ ground state at $\gamma \geq 25^\circ$ in this nucleus (the calculated point, shown by the open square, is drawn at $\gamma \approx 16.5^\circ$ and the experimental point, shown by filled square, is drawn at $\gamma \approx 25^\circ$).

The calculations of Ref. [5] performed at $\gamma = 16.5^\circ$ suggest the presence of a $3/2^+$ band at low energy in ^{107}Mo ,

TABLE II. Values of triaxial-deformation γ reported in the literature for neutron-rich Nb, Mo, and Tc isotopes.

Nucleus	γ deformation	Reference
^{105}Nb	12.3°	[26]
^{104}Mo	19.6°	[5]
^{105}Mo	17°	[5]
^{106}Mo	18.6°	[5]
^{107}Mo	16.5°	[5]
^{107}Mo	18°	[21]
^{108}Mo	23.4°	[5]
^{105}Tc	19°	[27]
^{106}Tc	-21°	[28]
^{107}Tc	19°	[27]
^{107}Tc	19°	[24]
^{107}Tc	22.5°	[29]
^{107}Tc	$22.5^\circ, 25^\circ$	[30]
^{109}Tc	$18^\circ, 23^\circ$	[29]
^{109}Tc	20°	[24]
^{109}Tc	22.5°	[31]
^{109}Tc	-30°	[32]
^{111}Tc	25°	[25]

analogous to the $3/2^+$ band observed in ^{105}Mo , which fits well the systematics of Fig. 9. However, the $3/2^+$ band in ^{107}Mo , reported in Ref. [4] to which the calculations of Ref. [5] were adjusted, has now been placed in the $1/2^+$ ground-state band. This agrees with the new energy systematics of Fig. 9, which does not predict any $3/2^+$ prolate band at low excitation energy neither in ^{107}Mo nor in ^{109}Mo . This is consistent with

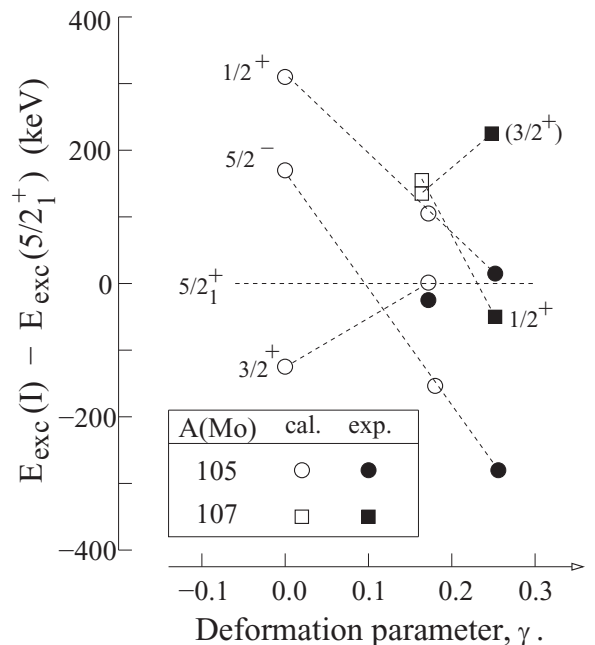


FIG. 11. The evolution of the calculated (open symbols) s.p. energies [5] in function of the γ deformation in Mo isotopes, drawn relative to the $5/2^+$ level. Filled symbols show positions of experimental levels, relative to the experimental $5/2^+$ level [1,5].

the larger γ deformation in the two nuclei. One sees in Fig. 11 that the $3/2^+$ energy is growing with the increasing γ in ^{105}Mo . With the same trend in ^{107}Mo a γ value larger than 16.5° is needed to reproduce the $3/2^+$ level in this nucleus, tentatively proposed at 543.8 keV.

The clear presence of triaxial deformation in odd- A , neutron-rich Mo isotopes suggests possible improvements of the theoretical systematics [13], redrawn in this paper in Figs. 3 and 10. The main deficiency of the calculations, mentioned by the authors [13], is the preservation of axial symmetry. This may explain why the calculated systematics in Fig. 3 is close to the experimental systematics for the odd- A Zr isotopes shown in Fig. 2 but differs from the experimental systematics for the odd- A Mo isotopes. In the Mo isotopes, there is clear triaxial deformation whereas, in the Zr isotopes, this effect only starts to emerge [33]. As suggested by Fig. 11, the inclusion of triaxiality in Mo isotopes may lower the energy of the $5/2^-$ orbital improving its too high excitation energy. At the same time, the higher population of this orbital may delay the population of the oblate configurations, which appears at too low a neutron number as seen in Fig. 11.

V. SUMMARY

Following the observation of the new, $1/2^+$ ground state in the ^{107}Mo nucleus [1], we searched for an analogous effect in ^{109}Mo , hinted by the recent studies [1,5,7]. Regular energy systematics developed and used in this paper provided

accurate predictions for the low-energy excitations in ^{107}Mo and ^{109}Mo , suggesting the new $1/2^+$ ground state in ^{109}Mo and a new $5/2^-$ level in ^{107}Mo . We used triple- γ coincidences from spontaneous fission of ^{248}Cm and ^{252}Cf , measured using Eurogam2 and Gammasphere arrays of anti-Compton spectrometers, respectively, to search for these levels. In this paper, we confirm the new $1/2^+$ ground state of ^{107}Mo , proposed recently [1], and establish the isomeric character of the $5/2^+$ first excited state in ^{107}Mo . The new $5/2^-$ head is found for the negative-parity band in ^{107}Mo . The new $1/2^+$ ground state is established in ^{109}Mo , and the isomeric character of the $5/2_1^+$ level in ^{109}Mo is proposed. Low-energy excitations in Mo isotopes are interpreted and compared to calculations reported in the literature. The comparison of calculated and experimental excitation energies in chains of Mo and Tc isotopes suggests that the γ deformation of ^{107}Mo is higher than reported before. The present results suggest a shape transition from prolate to oblate deformation at $N \geq 67$, confirming our early suggestion for such an effect [34].

ACKNOWLEDGMENTS

The authors are indebted for the use of a ^{248}Cm source to the Office of Basic Energy Sciences, U.S. Department of Energy, through the transplutonium element production facilities at the Oak Ridge National Laboratory. Argonne National Laboratory's work was supported by the U.S. Department of Energy, Office of Science, Office of Nuclear Physics under Contract No. DE-AC0206CH11357.

-
- [1] J. Kurpeta, A. Płochocki, W. Urban, A. Abramuk, L. Canete, T. Eronen, A. Fijałkowska, S. Geldhof, K. Gotowicka, A. Jokinen, A. Kankainen, I. D. Moore, D. Nesterenko, H. Penttilä, I. Pohjalainen, M. Pomorski, M. Reponen, S. Rinta-Antila, A. de Roubin, T. Rząca-Urban, M. Vilén, and J. Wiśniewski, *Phys. Rev. C* **100**, 034316 (2019).
- [2] M. A. C. Hotchkis, J. L. Durell, J. B. Fitzgerald, A. S. Mowbray, W. R. Phillips, I. Ahmad, M. P. Carpenter, R. V. F. Janssens, T. L. Khoo, E. F. Moore, L. R. Morss, Ph. Benet, and D. Ye, *Nucl. Phys. A* **530**, 111 (1991).
- [3] J. K. Hwang, A. V. Ramayya, J. H. Hamilton, L. K. Peker, J. Kormicki, B. R. S. Babu, T. N. Ginter, G. M. Ter-Akopian, Y. T. Oganessian, A. V. Daniel, W. C. Ma, P. G. Varmette *et al.*, *Phys. Rev. C* **56**, 1344 (1997).
- [4] W. Urban, T. Rząca-Urban, J. A. Pinston, J. L. Durell, W. R. Phillips, A. G. Smith, B. J. Varley, I. Ahmad, and N. Schulz, *Phys. Rev. C* **72**, 027302 (2005).
- [5] J. A. Pinston, W. Urban, C. Droste, T. Rząca-Urban, J. Genevey, G. Simpson, J. L. Durell, A. G. Smith, B. J. Varley, and I. Ahmad, *Phys. Rev. C* **74**, 064304 (2006).
- [6] J. Blachot, *Nucl. Data Sheets* **62**, 709 (1991).
- [7] D. Kameda, T. Kubo, T. Ohnishi, K. Kusaka, A. Yoshida, K. Yoshida, M. Ohtake, N. Fukuda, H. Takeda, K. Tanaka, N. Inabe, Y. Yanagisawa, Y. Gono, H. Watanabe, H. Otsu, H. Baba, T. Ichihara, Y. Yamaguchi, M. Takechi *et al.*, *Phys. Rev. C* **86**, 054319 (2012).
- [8] J. Kurpeta, W. Urban, A. Płochocki, J. Rissanen, V.-V. Elomaa, T. Eronen, J. Hakala, A. Jokinen, A. Kankainen, P. Karvonen, I. D. Moore, H. Penttilä, S. Rahaman, A. Saastamoinen, T. Sonoda, J. Szerypo, C. Weber, and J. Äystö, *Phys. Rev. C* **82**, 027306 (2010).
- [9] J. Kurpeta, A. Płochocki, W. Urban, T. Eronen, A. Jokinen, A. Kankainen, V. S. Kolhinen, I. D. Moore, H. Penttilä, M. Pomorski, S. Rinta-Antila, T. Rząca-Urban, and J. Wiśniewski, *Phys. Rev. C* **98**, 024318 (2018).
- [10] W. Urban, T. Rząca-Urban, J. Wiśniewski, I. Ahmad, A. G. Smith, and G. S. Simpson, *Phys. Rev. C* **99**, 064325 (2019).
- [11] W. Urban, J. A. Pinston, T. Rząca-Urban, E. Wolska, J. Genevey, G. S. Simpson, A. G. Smith, J. L. Durell, B. Varley, and I. Ahmad, *Phys. Rev. C* **79**, 067301 (2009).
- [12] Evaluated nuclear structure data file and experimental unevaluated nuclear data list nuclear structure databases of the Nuclear Data Center, Brookhaven National Laboratory [<http://www.nndc.bnl.gov/2020>].
- [13] R. Rodriguez-Guzman, P. Sarriguren, and L. M. Robledo, *Phys. Rev. C* **82**, 044318 (2010).
- [14] P. J. Nolan, F. A. Beck, and D. B. Fossan, *Annu. Rev. Nucl. Part. Sci.* **44**, 561 (1994).
- [15] I-Yang Lee, *Nucl. Phys. A* **520**, c641 (1990).
- [16] W. Urban, M. Czerwiński, J. Kurpeta, T. Rząca-Urban, J. Wiśniewski, T. Materna, Ł. W. Iskra, A. G. Smith, I. Ahmad, A. Blanc, H. Faust, U. Köster, M. Jentschel, P. Mutti, T. Soldner, G. S. Simpson, J. A. Pinston, G. de France, C. A. Ur, V.-V. Elomaa, T. Eronen, J. Hakala, A. Jokinen, A. Kankainen, I. D. Moore, J. Rissanen *et al.*, *Phys. Rev. C* **96**, 044333 (2017).
- [17] D. Patel, A. G. Smith, G. S. Simpson, R. M. Wall, J. F. Smith, O. J. Onakanmi, I. Ahmad, J. P. Greene, M. P. Carpenter, T. Lauritsen, C. J. Lister, R. F. Janssens, F. G. Kondev,

- D. Seweryniak, B. J. P. Gall, O. Dorveaux, and B. Roux, *J. Phys. G: Nucl. Part. Phys.* **28**, 649 (2002).
- [18] W. Urban, C. Droste, T. Rzača-Urban, A. Złomaniec, J. L. Durell, A. G. Smith, B. J. Varley, and I. Ahmad, *Phys. Rev. C* **73**, 037302 (2006).
- [19] T. Kibédi, T. W. Burrows, M. B. Trzhaskovskaya, P. M. Davidson, and C. W. Nestor, Jr., *Nucl. Instrum. Methods Phys. Res., Sect. A* **589**, 202 (2008) [computer code available in “Tools and Publications” at www.nndc.bnl.gov].
- [20] I. Ahmad and W. R. Phillips, *Rep. Prog. Phys.* **58**, 1415 (1995).
- [21] J. Marcellino, E. H. Wang, C. J. Zachary, J. H. Hamilton, A. V. Ramayya, G. H. Bhat, J. A. Sheikh, A. C. Dai, W. Y. Liang, F. R. Xu, J. K. Hwang, N. T. Brewer, Y. X. Luo, J. O. Rasmussen, S. J. Zhu, G. M. Ter-Akopian, and Y. T. Oganessian, *Phys. Rev. C* **96**, 034319 (2017); **102**, 029902(E) (2020).
- [22] C. Goodin, A. V. Ramayya, J. H. Hamilton, N. J. Stone, A. V. Daniel, K. Li, S. H. Liu, J. K. Hwang, Y. X. Luo, J. O. Rasmussen, and S. J. Zhu, *Phys. Rev. C* **80**, 014318 (2009).
- [23] R. A. Meyer, E. Monnard, J. A. Pinston, F. Schussler, B. Pfeiffer, I. Ragnarsson, H. Lawin, G. Lhersonneau, and K. Sistemich, *Nucl. Phys. A* **439**, 510 (1985).
- [24] J. Kurpeta, W. Urban, A. Płochocki, J. Rissanen, J. A. Pinston, V.-V. Elomaa, T. Eronen, J. Hakala, A. Jokinen, A. Kankainen, I. D. Moore, H. Penttilä, A. Saastamoinen, C. Weber, and J. Äystö, *Phys. Rev. C* **86**, 044306 (2012).
- [25] J. Kurpeta, W. Urban, A. Płochocki, J. Rissanen, J. A. Pinston, V.-V. Elomaa, T. Eronen, J. Hakala, A. Jokinen, A. Kankainen, P. Karvonen, I. D. Moore, H. Penttilä, A. Saastamoinen, C. Weber, and J. Äystö, *Phys. Rev. C* **84**, 044304 (2011).
- [26] H. J. Li, S. J. Zhu, J. H. Hamilton, A. V. Ramayya, J. K. Hwang, Y. X. Liu, Y. Sun, Z. G. Xiao, E. H. Wang, J. M. Eldridge, Z. Zhang, Y. X. Luo, J. O. Rasmussen, I. Y. Lee, G. M. Ter-Akopian, A. V. Daniel, Y. T. Oganessian, and W. C. Ma, *Phys. Rev. C* **88**, 054311 (2013).
- [27] G. Simpson, J. Genevey, J. A. Pinston, U. Köster, R. Orlandi, A. Scherillo, and I. A. Tsekhanovich, *Phys. Rev. C* **75**, 027301 (2007).
- [28] L. Gu, S. J. Zhu, J. H. Hamilton, A. V. Ramayya, J. K. Hwang, Y. X. Luo, J. O. Rasmussen, K. Li, I. Y. Lee, Q. Xu, X.-L. Che, E. Y. Yeoh, J.-G. Wang, H.-B. Ding, and Y.-Y. Yang, *Chin. Phys. C* **33**, 182 (2009).
- [29] W. Urban, J. A. Pinston, T. Rzača-Urban, J. Kurpeta, A. G. Smith, and I. Ahmad, *Phys. Rev. C* **82**, 064308 (2010).
- [30] T. W. Hagen, A. Görgen, W. Korten, L. Greife, M.-D. Salsac, F. Farget, T. Braunroth, B. Bruyneel, I. Celikovic, E. Clément, G. de France *et al.*, *Eur. Phys. J. A* **54**, 50 (2018).
- [31] Y. X. Luo, J. O. Rasmussen, J. H. Hamilton, A. V. Ramayya, J. K. Hwang, S. J. Zhu, P. M. Gore, S. C. Wu, I. Y. Lee, P. Fallon, T. N. Ginter, G. M. Ter-Akopian, A. V. Daniel, M. A. Stoyer, R. Donangelo, and A. Gelberg, *Phys. Rev. C* **70**, 044310 (2004).
- [32] L. Gu, S. J. Zhu, J. H. Hamilton, A. V. Ramayya, J. K. Hwang, S. H. Liu, J. G. Wang, Y. X. Luo, J. O. Rasmussen, I. Y. Lee, Q. Xu, E. Y. Yeoh, and W. C. Ma, *Chin. Phys. Lett.* **27**, 062501 (2010).
- [33] W. Urban, T. Rzača-Urban, J. Wiśniewski, A. G. Smith, G. S. Simpson, and I. Ahmad, *Phys. Rev. C* **100**, 014319 (2019).
- [34] W. Urban, T. Rzača-Urban, J. L. Durell, A. G. Smith, and I. Ahmad, *Eur. Phys. J. A* **24**, 161 (2005).